



Development of a Test Rig to Measure the EM-Susceptibility of an Unmanned Aerial Vehicle

Felix Burghardt*, Heyno Garbe

Institute of Electrical Engineering and Measurement Technology, Leibniz Universität Hannover, Germany,

<http://www.geml.uni-hannover.de>

Abstract

Unmanned Aerial Vehicles (UAV) become more and more part in our daily lives. They might be influenced by electromagnetic fields during their flight, which can cause serious safety problems. Therefore it is a matter of interest to know the electromagnetic interference immunity of an UAV. This paper describes a test rig setup, which is able to investigate the reaction of an UAV and its subsystems during the exposure to electromagnetic signals. It is also possible, to get a better understanding of the relations and dependencies between several subsystems of an UAV and the complete system. The test rig has a modular character, so it is simple to surveil the rotor frequency of all rotors or the data stream of the Flight Control Board (FCB). It was considered to keep the intervention of the Device Under Test (DUT) for all measurements as low as possible. It is also possible to examine a DUT during an electric field strength of up to $70 \frac{kV}{m}$, without disturbing the test rig itself. The analysis of this complex system leads to the conclusion, that the interference threshold of an UAV mainly depends on the interference threshold of the FCB.

1 Introduction

In the last years, the amount of Unmanned Aerial Vehicles (UAV) increased rapidly. UAVs, especially multicopters, become more and more popular in private or commercial matters. There are different types of multicopters (quadcopter, hexacopter, etc.), but common endeavor for all multicopters is a low dead weight.

A high electromagnetic interference immunity is normally opposed to a low weight. The higher weight is caused by electromagnetic shielding so for multicopters, it is important to only have a sufficient shielding instead of a perfect shielding.

It is of great interest which component or subsystem is most sensitive of the complete system. Therefore it is only necessary to shield this single component against electromagnetic interferences, to achieve a sufficient protection of an UAV. This could lead in further measurements to only examine one or a small amount of subsystems and not the complete system.

For a better understanding of the dependencies between subsystems, it is primarily important to consider the behavior of a single subsystem. After that, it is possible to draw conclusions to the complete system.

For this purpose a test rig is needed, which is able to:

- measure rotor frequencies and data stream of the Flight Control Board (FCB)
- operate accurate in an environment with an electric field strength of $70 \frac{kV}{m}$
- adjust measuring instruments after a detected incident automatically

Hence, the paper is structured as follows. At first, the structure of a multicopter is presented. The comprehension of the structure is important, to setup the test rig. This approach is described in 3. Starting from single subsystems to the complete system, the performed measurements by the test rig are presented in section 4.

2 Structure of a multicopter

The complex system "multicopter" can be structured into different subsystems. In figure 1, the block diagram of the multicopter "DJI Flame Wheel F550" is presented. On the left side, an antenna receives the Radio Frequency (RF) signal from the ground control and forwards this signal to the Remote Control Board (RCB). The RCB transforms the RF signal into a Pulse-Width Modulation (PWM) signal. After that, the Flight Control Board (FCB) calculates six control signals for the Motor Drive Boards (MDB). All control signals are based on the input signal and the integrated Inertial Measurement Unit (IMU). Depending on these control signals, the motor drivers generate an AC signal to control the Brushless (BL) motors.

A Lithium polymer (LiPo) battery provides all components of a multicopter with power. To protect the LiPo battery, a Power Management Unit (PMU) is surveilling the voltage. Separate from the IMU, the FCB is able to receive an external GPS and compass signal. These informations can also be used by the FCB for improving the precision. At last, a

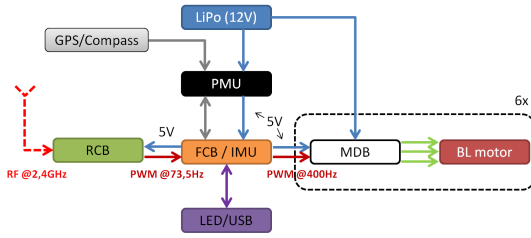


Figure 1. Block diagram of the multicopter "DJI Flame-Wheel"

LED module with an integrated USB port is able to connect directly to the FCB. With this module, a direct link to the inside of the FCB is possible.

It should be mentioned, that the FCB ("Naza-M V2" from DJI) has different operation modes. In this paper, two modes are examined:

- Manual mode: Multicopter uses only a small amount of sensors
- Attitude mode: Multicopter is able to stabilize the attitude. This mode needs more sensor informations

Because it was not possible to inject a RF Signal into the measurement chamber, the "GPS Mode" was not regarded.

Potthast [1] introduced the Fault Tree Analysis (FTA) of an UAV in his tutorial. The loss of an UAV is caused by a malfunction of the motor frequency. This can be caused by a malfunction inside the components RCB, FCB or MDB respectively between these components (coupling in cables). Because of the missing injection possibility, it makes no sense to surveil the RCB. Three system were build:

- Subsystem "MDB": Contains LiPo, one MDB and one BL motor
- Subsystem "FCB": Contains LiPo, PMU, FCB and in some iterations the GPS module and/or LED module
- Complete System: Contains LiPo, PMU, FCB, GPS module, LED module, six MDBs and six BL motors

3 Test rig

The test rig can be divided into a hardware and a software part. Primarily, the hardware part will be described. For better understanding, figure 2 presents all used components and their dependencies.

In a GTEM-Cell, the Device Under Test (DUT) is getting placed and connected with fibre optic transmitters and receivers. The DUT can receive control signals from the test rig computer, but transmits the analysis signals to the data

logger ("Yokogawa DL 750P"). This measurement instrument plots the complete measuring series and transmits it to the computer. The computer is able to control all measurement instruments (e.g. change parameters). After the external trigger gets a start signal, it primarily starts the data logger, waits for a fixed time and then activates the signal generator. The signal generator generates a fixed amount of pulses for a fixed time ("burst mode"). These pulses are used by the last signal generator. It is possible to use any signal generator (for continuous waves, pulses, etc.) until there is a trigger input. In this paper, the pulse generator "PBG3" respectively "PBG7" from Kentech was used, which creates double exponential pulses with a maximum amplitude of 13 kV respectively 40 kV. The PGB3/7 is connected to the GTEM-Cell so that an electromagnetic field propagates.

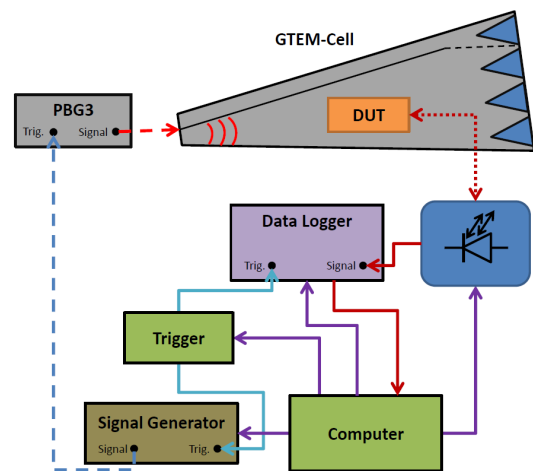


Figure 2. Block Diagram of the test rig with all used instruments

To control the test rig, a test rig software was developed. The whole control is based on LabVIEW from National Instruments. A logic is implemented so that after every measurement the software checks the complete measuring data for disturbances. The disturbances are classified by Sabath [2]. In this paper, the classification by Duration was used. That means, it was surveilled, if and how long the measurement signals vary from the normal state.

If the test rig detects no disruptions, the energy brought into the GTEM-Cell should be increased for the next measurement. This happens by increasing the amount of pulses generated by signal generator. However, if the test rig detects a disturbance, the disruption gets classified and depending on the error level, the measuring series is terminated. After that, the measurement will start with the lowest amount of pulses again.

Every measurement gets saved on a hard drive, including a measurement log. That simplifies an automatic evaluation and the comparison of different measurement parameters.

There are three different setups of the test rig:

- Subsystem "MDB": Input(1x PWM@400 Hz), Output(1x rotor frequency)
- Subsystem "FCB": Input(4x PWM@73.5 Hz), Output(6x PWM@400 Hz)
- Complete System: Input(4x PWM@73.5 Hz), Output(6x rotor frequency)

For transmitting and receiving PWM signals, fibre optic transmitters respectively receivers and for detecting the rotor frequency, self constructed fork light barrier are used. Figure 3 shows gray fork light barriers on top of and six black fibre optic receivers in front of the multicopter.

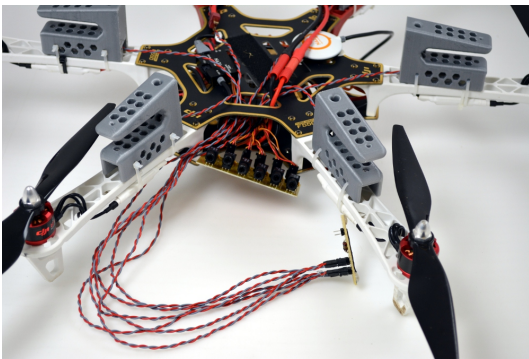


Figure 3. Fork light barriers and fibre optics receiver, mounted on the DUT

Changes of the test rig caused by different DUTs are simple, because only the software settings must be adjusted. If these profiles are saved, the user has only to load the fitting profile for the DUT.

4 Measurements

All DUTs were surveilled using different parameters during the exposure to electromagnetic signals. Different parameters are e.g. electric field strength, angle of entry, mode of the FCB and amount of periphery (GPS, LED). Every parameter setting was repeated 20 times, with 10 different pulse repetition rates (400 - 4000 pulses). The results of every DUT are presented in the following subsections.

4.1 Subsystem: "MDB"

By far, the subsystem "MDB" needs the highest electric field strength of all DUTs, until a disruption could be detected. The electric field strength has a range from $40 \frac{kV}{m}$ up to $70 \frac{kV}{m}$. It depends on the direction of the power supply cable and power consumption of the DUT. If the power supply cable orientated parallel to the propagation direction, a higher electric field strength is needed as if the cable has a transverse orientation. Increasing the power consumption of the DUT, the subsystem is weakened against High-Power-Electro-Magnetic (HPEM) exposures vice versa.

4.2 Subsystem: "FCB"

An investigation of the subsystem "FCB" is very complex. It depends on a huge amount of parameters (44 different parameter settings were measured). Summarizing all results, it is determined an electric field strength of approximately $5.3 \frac{kV}{m}$, which is the minimum, where disturbances are detected. The susceptibility is strongly influenced by the angle of entry and the mode of operation. By choosing the attitude mode, disruptions and even failures of the DUT occur. With the same parameters but using the manual mode, no failures were detected. In general can be stated, the more periphery were added the more increases the vulnerability of the subsystem.

4.3 Complete System

The results of surveilling the complete system is a mix between both subsystems. On one side, disturbances get detected at an electric field strength of approximately $4.1 \frac{kV}{m}$. That is a lower field strength but it is closer to subsystem "FCB" than to subsystem "MDB". But on the other side, the disturbances are now not depending on the FCB mode. There is no difference if the complete system gets admitted during manual or attitude mode. Also, the complete system has the same behavior if the power consumption is increased.

During some measurements, the complete system gets a failure and the operator isn't able to control the system, after the exposition ends. Only a "hard reset" (manual switch of the LiPo battery) can reset the multicopter. During measurements of the subsystem "FCB", there are also failures, but the operator can always reset the FCB without disrupting the power supply.

5 Conclusion

A multicopter can be considered as a complex system. The idea, to examine only subsystems (because it simplifies the measuring) did not lead to desired results. With knowledge based on measurements on subsystem level, it is possible to approximate the vulnerable electric field strength of the complete system. For the examined multicopter, it is the Flight Control Board (FCB). However, a simple adaption of the behavior from subsystem level to complete system is not possible.

6 Acknowledgements

The authors would like to thank the Electromagnetic Effects and HPEM team at the Bundeswehr Research Institute for Protective Technologies and NBC Protection, Munster, 205 Germany, for their hospitality and reliable support in the EMC laboratory. The research work was funded by the same institute with contract number E/E590/CZ025/CF149. The authors would also like to thank Tim Peikert for his helpful contributions.

References

- [1] S. Potthast, "Tutorial: A brief Introduction on the Susceptibility of UAS against HPEM Threats". 2015 IEEE International Symposium on Electromagnetic Compatibility (EMC), Dresden, 2015
- [2] F. Sabath, "Classification of Electromagnetic Effects at System Level", pp. 325-333 in Ultra-Wideband, Short-Pulse Electromagnetics 10 Editors: Frank Sabath, Eric L. Mokole Springer Verlag 2010 ISBN: 978-1-4614-9499-7 (Print) 978-1-4614-9500-0 (Online)